

Exotic Θ^+ baryon production induced by a photon and a pion

Yongseok Oh,* Hungchong Kim,[†] and Su Hyoung Lee[‡]

Institute of Physics and Applied Physics, Yonsei University, Seoul 120-749, Korea

(Received 1 October 2003; published 28 January 2004)

We investigate the photoproduction of the $\Theta^+(1540)$ on a nucleon ($\gamma n \rightarrow K^-\Theta^+$, $\gamma p \rightarrow \bar{K}^0\Theta^+$) and the pion-induced Θ^+ production reaction on the proton ($\pi^- p \rightarrow K^-\Theta^+$). The total cross sections near threshold are estimated by using hadronic models with effective interaction Lagrangians and form factors that preserve the gauge invariance of the electromagnetic current. The photoproduction cross sections are found to be a few hundred nb, with the cross section on the proton being larger than that on the neutron. The pion-induced production cross section is found to be around a few hundred μb but sensitive to the $K^*N\Theta$ coupling whose value is not yet known. We also study the production cross section assuming that Θ^+ has negative parity. The cross sections are then found to be very suppressed compared to the case where Θ^+ has positive parity. Hence, the interpretation of the Θ^+ as an odd-parity pentaquark state seems to be disfavored from the estimates of the cross section for the photon-proton reaction from the SAPHIR experiment.

DOI: 10.1103/PhysRevD.69.014009

PACS number(s): 13.60.Rj, 13.60.-r, 13.75.Gx, 14.80.-j

I. INTRODUCTION

The recent interest in pentaquark exotic hadrons was triggered by the discovery of the $\Theta^+(1540)$ baryon by the LEPS Collaboration at SPring-8 [1], where the photon beam was used on a ^{12}C target to produce the pentaquark Θ^+ from the $\gamma n \rightarrow K^-\Theta^+$ reaction. The upper limit of its decay width (Γ_Θ) was estimated to be 25 MeV. The CLAS Collaboration at the Thomas Jefferson National Accelerator Facility used the photon-deuteron reaction to produce the Θ^+ and found the decay width to be less than 21 MeV [2]. The SAPHIR Collaboration used the photon-proton reaction ($\gamma p \rightarrow \bar{K}^0\Theta^+$), where the decay width is found to be less than 25 MeV [3]. The Θ^+ production with $\Gamma_\Theta \leq 9$ MeV was also reported in the kaon-neutron reaction ($K^+ n \rightarrow K^0 p$) by the DIANA Collaboration [4]. Recently the νN reaction was used to search for Θ^+ with $\Gamma_\Theta < 20$ MeV [5].

Although the quantum numbers of the $\Theta^+(1540)$ are still to be determined, the interpretation of it as being a pentaquark ($uudds$) state is solid because Θ^+ has positive strangeness ($S = +1$). Such a low-lying pentaquark state with a narrow width was first predicted in the chiral quark soliton model [6], although the existence of such exotic states was anticipated earlier in the study of the Skyrme model [7–9]. The recent experimental findings prompted a lot of theoretical reinvestigation of the pentaquark states including the pentaquark ($P_{\bar{Q}}$) with one heavy antiquark [10–17]. Subsequent theoretical investigations on the Θ^+ include approaches based on the constituent quark model [12,18–21], Skyrme model [8,9,22–25], QCD sum rules [26–28], chiral potential model [29], large N_c QCD [30], lattice QCD [31], and group theory approach [32]. The production of the Θ^+ was also discussed in relativistic nuclear collisions [33,34], where the number of the anti- $\Theta^+(1540)$ produced

are expected to be similar to that of the $\Theta^+(1540)$. However, the genuine structure of the Θ^+ is still to be clarified, e.g., it is not yet firmly established whether the Θ^+ forms an anti-decuplet with the Roper resonance [20], and its spin parity is not yet confirmed. On the other hand, Jaffe and Wilczek suggested diquark-diquark-antiquark nature of the Θ^+ in the antidecuplet plus octet representation of SU(3) [11]. In Ref. [35], the Θ^+ is even claimed to be a heptaquark state. In addition, Capstick *et al.* suggested Θ^+ as a member of isotensor pentaquark family [36], which is, however, doubted by the SAPHIR experiment.

In the midst of such confusion, one attempt is to assume certain quantum numbers for the Θ^+ and investigate its physical properties [37–40]. As a starting point to compare with experimental observations, it is important to investigate the production processes of the Θ^+ in the photon-induced and pion-induced reactions. Since the production processes are studied in the medium energy region, the hadronic description would be more appropriate than perturbative QCD. There have been studies in this direction, where a hadronic model with effective interaction Lagrangians was used to calculate the reaction cross sections. In Refs. [41,42], Liu and Ko estimated the cross sections of positive-parity Θ^+ production from photon-nucleon scattering and various meson-nucleon scatterings. The authors considered not only the two-body final states, but also three-body final states. They claimed that the cross sections are about 0.05 mb in pion-nucleon reaction, 40 nb in photon-proton reaction, and 280 nb in photon-neutron reaction [41]. The cross section for the photon-neutron reaction is claimed to be substantially larger than that for photon-proton reaction. The values are changed in their sequential work [42], which includes the contributions from the K^* exchanges in the photon-nucleon reactions. However, this work does not take into account the tensor coupling of the photon-nucleon and photon- Θ^+ interactions. In particular, they did not include the s -channel diagrams and the anomalous magnetic momentum terms in the u channels in photoproduction reaction, which were shown to be important in Ref. [43]. In addition, the final results

*Electronic address: yoh@phya.yonsei.ac.kr

[†]Electronic address: hung@phya.yonsei.ac.kr

[‡]Electronic address: suhong@phya.yonsei.ac.kr

were obtained by multiplying a form factor that is a function of the center-of-mass energy only. In Ref. [43], Nam *et al.* considered $\gamma n \rightarrow K^- \Theta^+$ process using pseudoscalar and pseudovector couplings as well as a hybrid model. Then the authors included the effects of the form factors by dividing the cross section by an overall energy-independent constant, whose value is obtained from a similar prescription to match the theoretical Born term estimate of the total cross section for kaon photoproduction to the experimental data. They also considered the case where the quantum numbers of the Θ^+ are $J^P = \frac{1}{2}^-$. Then they found that the Θ^+ production cross section in photon-neutron reaction near threshold is 14–20 nb for negative-parity Θ^+ and 100–240 nb for the positive-parity Θ^+ . However, in their work, the K^* exchange was not considered and the assumption that the Θ^+ production cross section can just be divided by a constant factor is unjustified. Experimentally, the only information available for any production cross sections comes from the SAPHIR Collaboration [3], which claims that the cross section for $\gamma p \rightarrow \bar{K}^0 \Theta^+$ is similar to that of ϕ photoproduction and is of the order of 200 nb near threshold, which is to be confirmed by further analyses [44].

In this work, we perform a more consistent calculation on the photoproduction of the Θ^+ from the nucleon targets and on the pion-induced production from the proton target. The latter reaction is of particular interest since the current KEK experiment searching for the Θ^+ is using this reaction. Such a reaction can also be studied with the recent pion beam facility at GSI. Several improvements are included in our work compared with previous hadronic model calculations in Refs. [41–43]. To investigate the sensitivity on the possible form factors, we employ form factors that are functions of the transferred momenta and compare the results with the previous ones that use different prescriptions for the form factors. We also include the K^* exchanges in the t channel in all relevant reactions. As we will show, the contributions from the K^* exchange are appreciable in all the production reactions considered and in fact dominant in the pion-induced reaction. Another important question that we address is the parity of the Θ^+ , which is not yet settled. For example, Refs. [19,26,28,31] suggest that the parity of the Θ^+ is preferably odd, while many other approaches including soliton models claim or assume it to be even. Therefore we will first present the results assuming that the $\Theta^+(1540)$ is an isosinglet, spin-1/2 baryon with positive parity, and then the results with assuming that the Θ^+ has negative parity will be compared and discussed.

II. $\gamma n \rightarrow K^- \Theta^+$ AND $\gamma p \rightarrow \bar{K}^0 \Theta^+$

The Feynman diagrams of Θ^+ photoproduction from the neutron and proton targets are shown in Figs. 1 and 2. The momenta of the incoming photon, the nucleon, the outgoing K , and the Θ are k , p , q , and p' , respectively. The Mandelstam variables are $s = (k+p)^2$, $t = (k-q)^2$, and $u = (p-q)^2$. It should be noted that we have neglected the s -channel diagrams in which the intermediate baryon is the nucleon resonance, including the Roper resonances or the nonstrange analog of the Θ^+ that could be the Roper

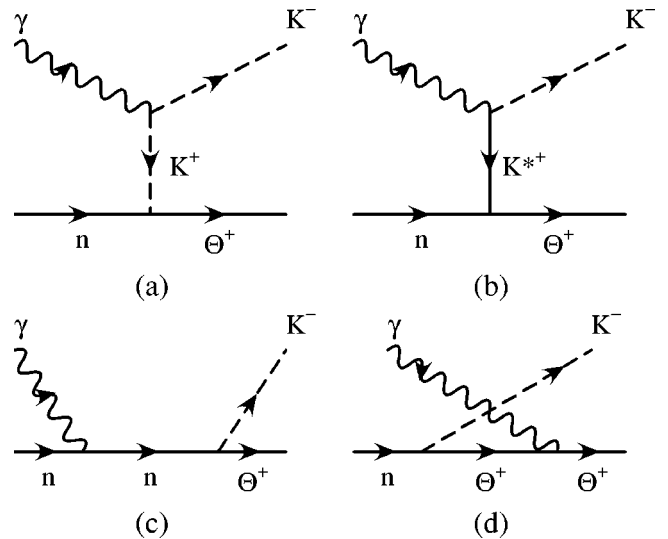


FIG. 1. Diagrams for the $\gamma n \rightarrow K^- \Theta^+$ reaction.

$N(1710)$ [6,11]. Such approximations should be good enough in a first attempt calculation, where at least all the ground state nucleon, pseudoscalar, and vector mesons are consistently included.

For the parity of the Θ^+ , we note that the chiral quark soliton model predicts even parity. This seems to be consistent with the Skyrme model results on the pentaquark states containing one heavy antiquark. In that model, the lowest state of the pentaquark with one heavy antiquark and four light u, d quarks has $I=0$ and $J^P = \frac{1}{2}^+$, while the first excited state has $I=0$ and $J^P = \frac{1}{2}^-$, and the $I=1$ pentaquarks are higher states [16]. The Θ^+ with $J^P = \frac{1}{2}^+$ is also favored by a recent Skyrme model study [25] and a constituent quark model study [45]. Thus, we first assume that the Θ^+ has positive parity, postponing the negative-parity case to Sec. IV. Then the effective Lagrangians read

$$\begin{aligned} \mathcal{L}_{\gamma K K} &= ie A_\mu (K^- \partial^\mu K^+ - \partial^\mu K^- K^+), \\ \mathcal{L}_{K N \Theta} &= -ig_{K N \Theta} (\bar{\Theta} \gamma_5 K^+ n - \bar{\Theta} \gamma_5 K^0 p) + \text{H.c.}, \\ \mathcal{L}_{\gamma \Theta \Theta} &= -e \bar{\Theta} \left[A_\mu \gamma^\mu - \frac{\kappa_\Theta}{2M_\Theta} \sigma_{\mu\nu} \partial^\nu A^\mu \right] \Theta, \\ \mathcal{L}_{\gamma N N} &= -e \bar{N} \left[A_\mu \gamma^\mu \frac{1 + \tau_3}{2} - \frac{1}{4M_N} \{ \kappa_p + \kappa_n \right. \\ &\quad \left. + \tau_3 (\kappa_p - \kappa_n) \} \sigma_{\mu\nu} \partial^\nu A^\mu \right] N, \end{aligned} \quad (1)$$

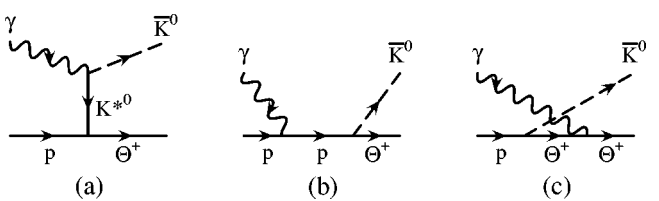


FIG. 2. Diagrams for the $\gamma p \rightarrow \bar{K}^0 \Theta^+$ reaction.

where A_μ is the photon field and $N^T = (p, n)$. The anomalous magnetic moments of the proton and neutron are κ_p ($= 1.79$) and κ_n ($= -1.91$), respectively. Here we use the SU(3) Lagrangian for the phases of the $\Theta^+ KN$ interactions [46].

For the K^* exchange, we use

$$\begin{aligned} \mathcal{L}_{K^*K\gamma} &= g_{K^*K\gamma} \epsilon^{\mu\nu\alpha\beta} \partial_\mu A_\nu (\partial_\alpha K_\beta^{*-} K^+ + \partial_\alpha \bar{K}_\beta^{*0} K^0) + \text{H.c.}, \\ \mathcal{L}_{K^*N\Theta} &= -g_{K^*N\Theta} \bar{\Theta} \left(\gamma^\mu K_\mu^{*+} - \frac{\kappa_{K^*n\Theta}^T}{M_N + M_\Theta} \sigma^{\mu\nu} \partial_\nu K_\mu^{*+} \right) n \\ &+ g_{K^*N\Theta} \bar{\Theta} \left(\gamma^\mu K_\mu^{*0} - \frac{\kappa_{K^*p\Theta}^T}{M_N + M_\Theta} \sigma^{\mu\nu} \partial_\nu K_\mu^{*0} \right) p \\ &+ \text{H.c.} \end{aligned} \quad (2)$$

The coupling constants are determined as follows. The Lagrangian $\mathcal{L}_{KN\Theta}$ gives the decay width of $\Theta^+ \rightarrow KN$ as

$$\Gamma_{\Theta^+ \rightarrow K^+ n + K^0 p} = \frac{g_{KN\Theta}^2}{2\pi} \frac{|\mathbf{p}_K| (\sqrt{M_N^2 + \mathbf{p}_K^2} - M_N)}{M_\Theta}, \quad (3)$$

where M_N and M_Θ are the nucleon and Θ^+ mass, respectively, and \mathbf{p}_K is the momentum of the kaon in the Θ^+ rest frame. Thus, the coupling $g_{KN\Theta}$ can be estimated from the Θ^+ decay width. In Ref. [39], the decay ratio $\Gamma_{\Theta^+ \rightarrow K^+ n} / \Gamma_{\Theta^+ \rightarrow K^0 p}$ was shown to be dependent on the isospin of the Θ^+ . If the Θ^+ is an isosinglet, this ratio becomes one. Theoretically, the chiral soliton model of Ref. [6] predicted a very narrow width of less than 15 MeV. Later it was claimed to be about 5 MeV in an improved analysis of the same model [47]. This small decay width seems to be consistent with recent analyses on KN scattering that suggest a narrow width of a few MeV for the Θ^+ [48–51]. Experimentally, only the upper bound of the Θ^+ decay width is known, around 9–25 MeV. If we take the results of the chiral quark soliton model [47] and the KN scattering analyses [48–51], which is $\Gamma_{\Theta^+ \rightarrow KN} = 5\text{--}10$ MeV, we get

$$g_{KN\Theta} = 2.2\text{--}3.11. \quad (4)$$

This value is much smaller than $g_{K\Lambda}$, which is -16.0 to -10.6 , but rather close to $g_{K\Sigma}$, which is $3.1\text{--}4.6$ [52]. In this work, we use $g_{KN\Theta} = 2.2$ following Ref. [47]. The only undetermined parameter in Eq. (1) is κ_Θ , the anomalous magnetic moment of the Θ^+ , which should reveal the structure of the Θ^+ . In Ref. [43], the authors estimated κ_Θ in several models. For example, they obtained $\kappa_\Theta \sim -0.7$ in the diquark-diquark-antiquark picture of Jaffe and Wilczek [11], while $\kappa_\Theta \sim -0.4$ if the Θ^+ is a KN system. These values are different from the chiral quark soliton model that gives $\kappa_\Theta \sim +0.3$ [53]. In this work, we will treat κ_Θ as a free parameter and give the results in the range of $-0.7 < \kappa_\Theta < +0.7$.

The Lagrangians of Eq. (2) contain four coupling constants. The coupling $g_{K^*K\gamma}$ is estimated from the experimental data for K^* radiative decays. The decay width is given by

$$\Gamma_{K^* \rightarrow K\gamma} = \frac{g_{K^*K\gamma}^2}{12\pi} |\mathbf{p}_\gamma|^3. \quad (5)$$

Using the experimental values [54], we obtain $g_{K^*K\gamma} = 0.388 \text{ GeV}^{-1}$ for the neutral decay and $g_{K^*K\gamma} = 0.254 \text{ GeV}^{-1}$ for the charged decay. However, there is no information on the couplings $g_{K^*N\Theta}$, $\kappa_{K^*n\Theta}^T$, and $\kappa_{K^*p\Theta}^T$. Since the decay of the Θ^+ into K^*N is not kinematically allowed, we have to rely on the theoretical estimate, which is, however, not available until now. The only hint we have is that $g_{K^*N\Lambda} \sim -4.5$ and $g_{K^*N\Sigma} \sim -2.6$, which are smaller than $g_{K\Lambda}$ and $g_{K\Sigma}$ by a factor of 2.4–3.5 or 1.2–1.8 [55]. From this observation, we expect that $g_{K^*N\Theta}$ would be smaller than $g_{K\Lambda}$. However, their relative phase is still unfixed. Thus, we treat $g_{K^*N\Theta}$ as a free parameter and give the results by varying $g_{K^*N\Theta}$. We shall find that measuring the pion-induced process together with the photon-induced processes will give us a clue on the $g_{K^*N\Theta}$ coupling. The tensor couplings $\kappa_{K^*n\Theta}^T$ and $\kappa_{K^*p\Theta}^T$ should also be examined, but they will not be considered in this exploratory study.

The photoproduction amplitudes are in general written as

$$T = \varepsilon_\mu \bar{u}_\Theta(p') \mathcal{M}^\mu u_N(p), \quad (6)$$

where ε_μ is the photon polarization vector. With the effective Lagrangians above, it is straightforward to obtain the production amplitudes. For the $\gamma n \rightarrow K^- \Theta^+$ reaction (Fig. 1), we have

$$\mathcal{M}_{1(a)}^\mu = -\frac{ie g_{KN\Theta} (2q^\mu - k^\mu)}{t - M_K^2} \gamma_5 F_{1(a)}(s, t, u),$$

$$\mathcal{M}_{1(b)}^\mu = \frac{g_{K^*K\gamma} g_{K^*N\Theta}}{t - M_{K^*}^2} \epsilon^{\mu\nu\alpha\beta} k_\alpha q_\beta \gamma_\nu F_{1(b)}(s, t, u),$$

$$\begin{aligned} \mathcal{M}_{1(c)}^\mu &= -\frac{e \kappa_n}{2M_N} \frac{g_{KN\Theta}}{s - M_N^2} \gamma_5 (\not{k} + \not{p} + M_N) \\ &\times \sigma^{\mu\nu} k_\nu F_{1(c)}(s, t, u), \end{aligned}$$

$$\begin{aligned} \mathcal{M}_{1(d)}^\mu &= \frac{ie g_{KN\Theta}}{u - M_\Theta^2} \left(\gamma_\mu + \frac{i \kappa_\Theta}{2M_\Theta} \sigma^{\mu\nu} k_\nu \right) \\ &\times (\not{p} - \not{q} + M_\Theta) \gamma_5 F_{1(d)}(s, t, u), \end{aligned} \quad (7)$$

and for $\gamma p \rightarrow \bar{K}^0 \Theta^+$ (Fig. 2) we get

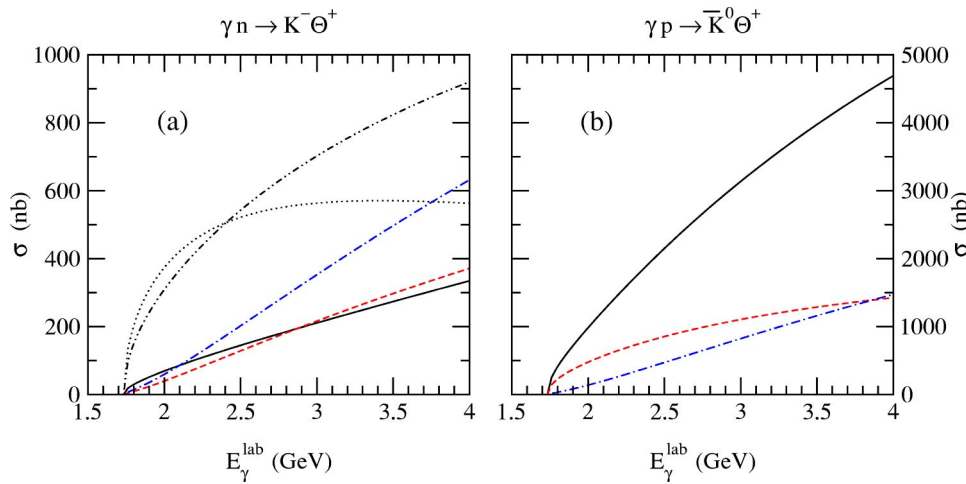


FIG. 3. Cross sections for (a) $\gamma n \rightarrow K^- \Theta^+$ and (b) $\gamma p \rightarrow \bar{K}^0 \Theta^+$ reactions without form factors. The dashed lines are the results without the K^* exchange and the dot-dashed lines are from the K^* exchange only. The solid lines are their sums. In (a), the dotted line is from the $(t+u)$ -channel and the dot-dot-dashed line is the s -channel result.

$$\begin{aligned}
 \mathcal{M}_{2(a)}^\mu &= -\frac{g_{K^*K\gamma}g_{K^*N\Theta}}{t-M_{K^*}^2} \epsilon^{\mu\nu\alpha\beta} k_\alpha q_\beta \gamma_\nu F_{2(a)}(s,t,u), \\
 \mathcal{M}_{2(b)}^\mu &= -\frac{ie g_{KN\Theta}}{s-M_N^2} \gamma_5 (\not{k} + \not{p} + M_N) \\
 &\quad \times \left(\gamma_\mu + \frac{i\kappa_p}{2M_N} \sigma^{\mu\nu} k_\nu \right) F_{2(b)}(s,t,u), \\
 \mathcal{M}_{2(c)}^\mu &= -\frac{ie g_{KN\Theta}}{u-M_\Theta^2} \left(\gamma_\mu + \frac{i\kappa_\Theta}{2M_\Theta} \sigma^{\mu\nu} k_\nu \right) \\
 &\quad \times (\not{p} - \not{q} + M_\Theta) \gamma_5 F_{2(c)}(s,t,u). \tag{8}
 \end{aligned}$$

Here we have multiplied form factors that take into account the structure of each vertex. The gauge invariance ($k \cdot \mathcal{M} = 0$) is then easily checked when all the form factors are set to one. In $\gamma n \rightarrow K^- \Theta^+$, the t -channel K^* exchange and the s -channel terms have gauge-invariant forms. The gauge-noninvariant part of the t -channel K exchange is canceled by that of the u -channel terms. In $\gamma p \rightarrow \bar{K}^0 \Theta^+$, the t -channel K^* exchange is gauge-invariant. And the sum of the s -channel and u -channel is gauge-invariant. But introducing different form factors at each vertex spoils gauge invariance. In Ref. [43], to keep gauge invariance and to include the effects of form factors, the cross section for $\gamma n \rightarrow K^- \Theta^+$ obtained from tree graphs is multiplied by 0.18. This factor is the average value of $\sigma_{\text{expt.}}/\sigma_{\text{theory}}$ in $\gamma p \rightarrow K^+ \Lambda$ reaction near threshold, where σ_{theory} contains the contribution from the Born terms only. However, in $\gamma p \rightarrow K^+ \Lambda$ there are other production mechanisms such as nucleon and hyperon resonances which interfere with the K^* exchanges and the nucleon Born terms [52,56,57]. Thus assuming the same suppression in Λ photoproduction and Θ^+ photoproduction is questionable and should be further tested. In Refs. [41,42], the authors used the same form factor for all channels, which is a function of \sqrt{s} only,

$$F(s) = \frac{\Lambda^2}{\Lambda^2 + \mathbf{q}_i^2}, \tag{9}$$

where \mathbf{q}_i is the three-momentum of the initial state particles in the center-of-mass (c.m.) frame,

$$\mathbf{q}_i^2 = \frac{1}{4s} \lambda(s, M_N^2, 0), \tag{10}$$

with $\lambda(x, y, z) = x^2 + y^2 + z^2 - 2(xy + yz + zx)$. Therefore, as the energy becomes larger, the cross section becomes smaller since $F(s)$ decreases rapidly with energy. Since the form of the form factors and the cutoff parameters should be justified by experimental data, measuring the total and differential cross sections should discern the form factor dependence of the cross sections.

In this work, we take another approach for the form factors. Motivated by the analyses of kaon photoproduction [52], we use the form factor [58]

$$F(r, M_{\text{ex}}) = \frac{\Lambda^4}{\Lambda^4 + (r - M_{\text{ex}}^2)^2}, \tag{11}$$

for each vertex. Here M_{ex} is the mass of the exchanged particle and r is the square of the transferred momentum. This has the correct on-shell condition that $F(r, M_{\text{ex}}) = 1$ at $r = M_{\text{ex}}^2$. However, introducing different form factors depending on the channels breaks gauge invariance. There are several recipes for restoring gauge invariance with the use of phenomenological form factors [59–61]. But the results depend on the employed form factors and the way to restore gauge invariance. In order to avoid any complication and to keep gauge invariance in a simple way, we use

$$\begin{aligned}
 F_{1(a)} &= F_{1(d)} = \{F(t, M_K)^2 + F(u, M_\Theta)^2\}/2, \\
 F_{1(b)} &= F(t, M_{K^*})^2, \quad F_{1(c)} = F(s, M_N)^2, \tag{12}
 \end{aligned}$$

and

$$\begin{aligned}
 F_{2(a)} &= F(t, M_{K^*})^2, \\
 F_{2(b)} &= F_{2(c)} = \{F(s, M_N)^2 + F(u, M_\Theta)^2\}/2. \tag{13}
 \end{aligned}$$

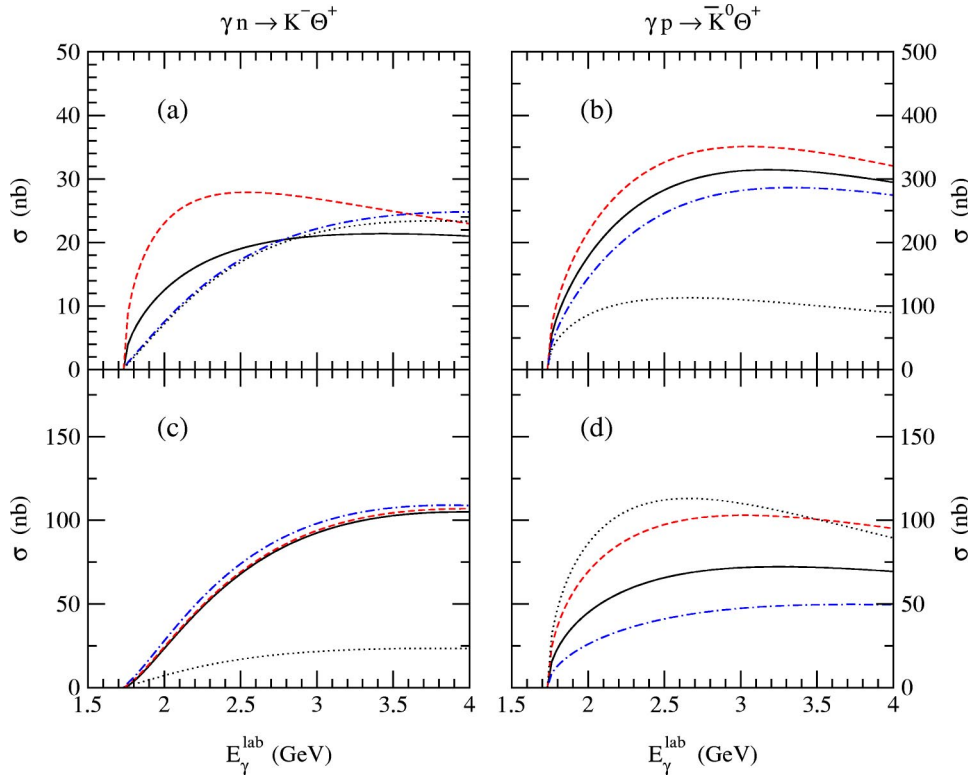


FIG. 4. Cross sections for (a,c) $\gamma n \rightarrow K^- \Theta^+$ and (b,d) $\gamma p \rightarrow \bar{K}^0 \Theta^+$ reactions with the form factors of Eq. (9) with $\Lambda = 0.75$ GeV. In (a,b), $g_{K^*N\Theta} = +2.2$ is used while $g_{K^*N\Theta} = -2.2$ in (c,d). The solid lines are obtained with $\kappa_\Theta = 0$, while the dashed and dot-dashed lines are with $\kappa_\Theta = +0.7$ and -0.7 , respectively. The dotted lines correspond to $g_{K^*N\Theta} = 0$.

This is an unsatisfactory aspect of this hadronic model approach, but it should be sufficient for this qualitative study. For comparison, we will give the results obtained with this form factor and those with the form factor of Eq. (9).

We are now ready to calculate the cross sections for Θ^+ photoproduction. In Fig. 3, the total cross sections for $\gamma n \rightarrow K^- \Theta^+$ and $\gamma p \rightarrow \bar{K}^0 \Theta^+$ are given without form factors. For this calculation we set $g_{K^*N\Theta} = g_{K^*N\Theta}$ and $\kappa_\Theta = 0$. In Fig. 3, the dashed lines are obtained without the K^* exchanges and the dot-dashed lines are with the K^* exchanges alone. The solid lines are their sums. This shows that the cross section for $\gamma p \rightarrow \bar{K}^0 \Theta^+$ is much larger than that for $\gamma n \rightarrow K^- \Theta^+$. This holds even in the absence of the K^* exchanges (dashed lines in Fig. 3). Several comments are in order. In the $\gamma n \rightarrow K^- \Theta^+$ reaction, there are strong (destructive) interference among the channels. In contrast to the assumption of Ref. [50], the contributions from the s and u channels are not suppressed. In both reactions, we found that the K^* exchange is not suppressed compared to the other production mechanisms although it strongly depends on the unknown coupling $g_{K^*N\Theta}$. It is interesting to note that the K^* exchange interferes destructively with the other amplitudes in $\gamma n \rightarrow K^- \Theta^+$ but constructively in $\gamma p \rightarrow \bar{K}^0 \Theta^+$. If the relative phase between $g_{K^*N\Theta}$ and $g_{K^*N\Theta}$ is changed, then the interference patterns are reversed. In this case, $\gamma n \rightarrow K^- \Theta^+$ has a larger cross section than $\gamma p \rightarrow \bar{K}^0 \Theta^+$ when $E_\gamma^{\text{lab}} < 2.5$ GeV. For $E_\gamma^{\text{lab}} > 2.5$ GeV, the cross section for $\gamma p \rightarrow \bar{K}^0 \Theta^+$ becomes larger and increases faster than that of $\gamma n \rightarrow K^- \Theta^+$.

We now investigate the form factor dependence of the cross sections. Given in Fig. 4 are the cross sections obtained

with the form factor prescription of Eq. (9) with $\Lambda = 0.75$ GeV. The upper graphs are obtained with $g_{K^*N\Theta} = +2.2$ and the lower ones are with $g_{K^*N\Theta} = -2.2$. In this figure, we also give the results by varying κ_Θ from -0.7 to $+0.7$. The energy dependence of the cross sections are similar for both the neutron and proton targets, which is expected from the form of the form factor (9). When $g_{K^*N\Theta} = +2.2$, the cross section for $\gamma p \rightarrow \bar{K}^0 \Theta^+$ is larger than that for $\gamma n \rightarrow K^- \Theta^+$ by a factor of 10. However, when $g_{K^*N\Theta} = -2.2$, the cross section for $\gamma n \rightarrow K^- \Theta^+$ is slightly larger. In order to see the contributions from the K^* exchange, we give the results without the K^* exchange with $\kappa_\Theta = 0$ (dotted lines in Fig. 4).

In Fig. 5, we present our results with the form factors of Eq. (11). Here the results without the K^* exchange and with $\kappa_\Theta = 0$ are also shown by the dotted lines. The upper graphs are obtained with $g_{K^*N\Theta} = +2.2$ and the lower ones with $g_{K^*N\Theta} = -2.2$. In this calculation we use the cutoff

$$\Lambda = 1.8 \text{ GeV}, \quad (14)$$

as fixed in the study of Λ photoproduction with the same form factor prescription [52]. We see that with this form factor the final results are not so sensitive to the phase of the $g_{K^*N\Theta}$ coupling, indicating the large contributions from the K^* exchanges. We notice that our results are consistent with the observation of the SAPHIR Collaboration that the cross section for $\gamma p \rightarrow \bar{K}^0 \Theta^+$ is about 200 nb in the photon energy range from 1.7 to 2.6 GeV, and it is similar to the cross section for ϕ photoproduction. For comparison, we give the total cross section for ϕ photoproduction in the literature [62] by the dot-dot-dashed lines in Figs. 5(b,d). This shows

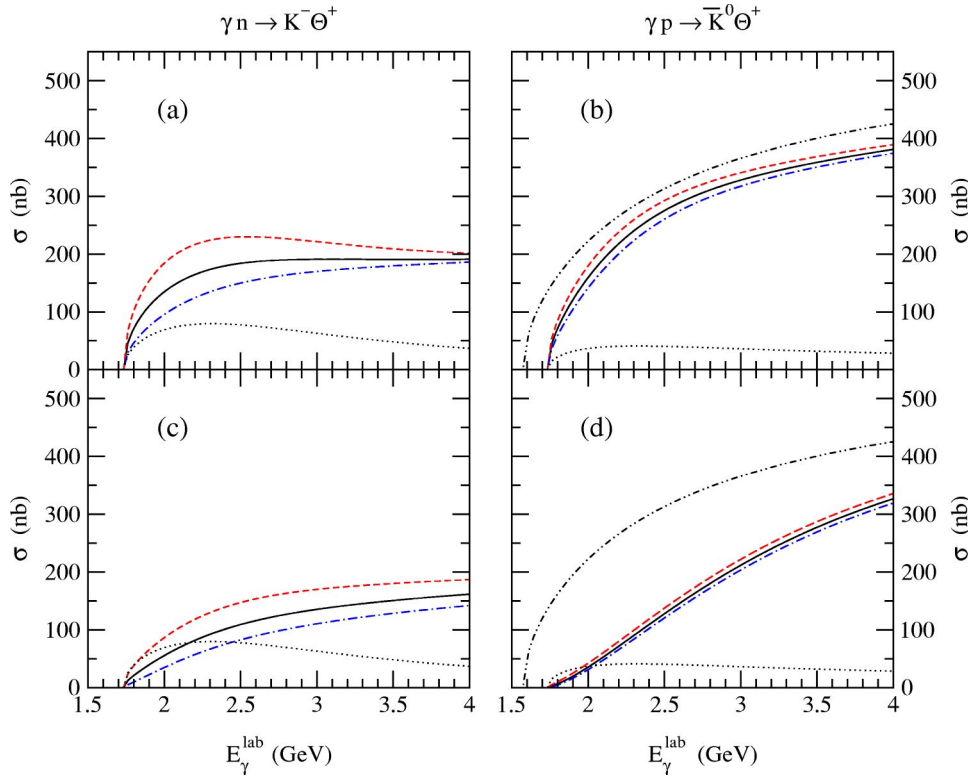


FIG. 5. Cross sections for (a,c) $\gamma n \rightarrow K^- \Theta^+$ and (b,d) $\gamma p \rightarrow \bar{K}^0 \Theta^+$ reactions with the form factors of Eq. (11). The notations are the same as in Fig. 4. In (b,d) the total cross section for ϕ photoproduction [62] is given by dot-dashed lines for comparison.

that the positive phase of $g_{K^*N\Theta}$ is favored by the SAPHIR experiment. In addition, the cross section for $\gamma p \rightarrow \bar{K}^0 \Theta^+$ is larger in most cases. We also find that the energy dependence of the cross sections for the two reactions is different. In $\gamma n \rightarrow K^- \Theta^+$, the cross section saturates as the energy increases, while it keeps increasing with the energy in $\gamma p \rightarrow \bar{K}^0 \Theta^+$. The κ_Θ dependence is negligible for the photon-proton reaction, while in the photon-neutron reaction the cross section nontrivially depends on κ_Θ . Since a different choice of the form factors gives different results, as can be seen in Figs. 4 and 5, it would be very useful to have measurements on the total and especially differential cross sections to justify a particular type of the form factors and to discriminate the role of each production channel.

III. $\pi^- p \rightarrow K^- \Theta^+$

We now turn to the pion-induced reaction, $\pi^- p \rightarrow K^- \Theta^+$, of which tree diagrams are shown in Fig. 6. Without the K^* exchange, only the s -channel diagram is allowed, which was considered in Ref. [41]. The possible u -channel diagram includes Θ' , whose minimal quark content should

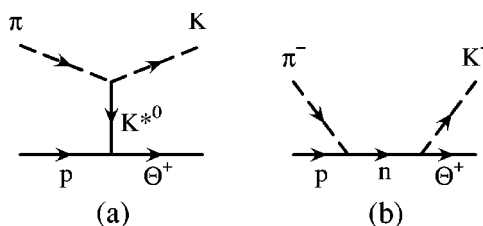


FIG. 6. Diagrams for $\pi^- p \rightarrow K^- \Theta^+$ reaction.

be $uuuds\bar{s}$. Such an exotic baryon may be a member of the isotensor pentaquarks as suggested by Ref. [36], but its existence seems to be disfavored by the SAPHIR experiment [3]. Thus we do not consider the u -channel diagrams in this study. Note also that the s -channel diagrams containing the nucleon resonances are neglected as in the Θ^+ photoproduction study of the preceding section. Furthermore, we will find that the t -channel K^* exchange is the most dominant process. For this calculation, in addition to $\mathcal{L}_{K^*N\Theta}$ of Eq. (2), we need the effective Lagrangian $\mathcal{L}_{K^*K\pi}$, which reads

$$\mathcal{L}_{K^*K\pi} = -ig_{K^*K\pi}\{\bar{K}\partial^\mu\pi K_\mu^* - \partial^\mu\bar{K}\pi K_\mu^*\} + \text{H.c.}, \quad (15)$$

where $K^T = (K^+, K^0)$, $\bar{K} = (K^-, \bar{K}^0)$, etc., and

$$\mathcal{L}_{\pi NN} = -ig_{\pi NN}\bar{N}\gamma_5\pi N, \quad (16)$$

with $\pi = \pi \cdot \tau$. The coupling constant $g_{K^*K\pi}$ fixed by the experimental data for $K^* \rightarrow K\pi$ decay,

$$\Gamma_{K^* \rightarrow K\pi} = \frac{g_{K^*K\pi}^2}{2\pi M_{K^*}^2} |\mathbf{p}_\pi|^3, \quad (17)$$

is $g_{K^*K\pi} = 3.28$, which is comparable to the SU(3) symmetry value, 3.02. We also use $g_{\pi NN}^2/(4\pi) = 14$.

The production amplitude of this reaction is written as

$$T = \bar{u}_\Theta(p') \mathcal{M} u_p(p), \quad (18)$$

where the diagrams of Fig. 6 give

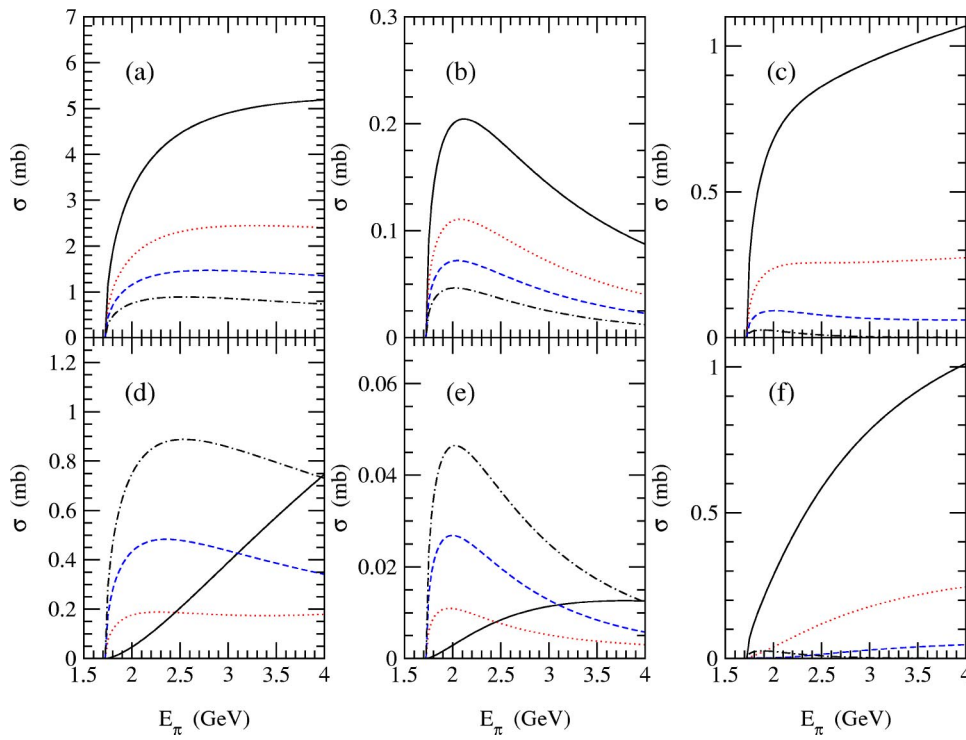


FIG. 7. Cross sections for $\pi^- p \rightarrow K^- \Theta^+$ (a,d) without form factors, (b,e) with the form factors of Eq. (9) with $\Lambda = 0.5$ GeV, and (c,f) with the form factors of Eq. (11) with $\Lambda = 1.8$ GeV. In (a,b,c), the solid, dotted, dashed, and dot-dashed lines are with $g_{K^*N\Theta} = -2.2, -1.1, -0.5$, and 0.0, respectively. In (d,e,f), the solid, dotted, dashed, and dot-dashed lines are with $g_{K^*N\Theta} = 2.2, 1.1, 0.5$, and 0.0, respectively.

$$\begin{aligned} \mathcal{M}_{6(a)} &= \frac{\sqrt{2}g_{K^*K\pi}g_{K^*N\Theta}}{t - M_{K^*}^2} \left\{ \not{k} + \not{q} + \frac{M_K^2 - M_\pi^2}{M_{K^*}^2}(\not{k} - \not{q}) \right\} \\ &\times F_{6(a)}(s, t, u), \\ \mathcal{M}_{6(b)} &= \frac{\sqrt{2}g_{K^*N\Theta}g_{\pi NN}}{s - M_N^2}(\not{k} + \not{p} - M_N)F_{6(b)}(s, t, u). \end{aligned} \quad (19)$$

As in photoproduction, we work with two choices of the form factors. First, following Ref. [41], we set

$$F_{6(a)}(s, t, u) = F_{6(b)}(s, t, u) = \frac{\Lambda^2}{\Lambda^2 + \not{q}_i^2}, \quad (20)$$

as in Eq. (9) with $\not{q}_i^2 = \lambda(s, M_N^2, M_\pi^2)/4s$. We also employ the covariant form factors as

$$F_{6(a)}(s, t, u) = F(t, M_{K^*})^2, \quad F_{6(b)}(s, t, u) = F(s, M_N)^2, \quad (21)$$

where $F(r, M)$ is given in Eq. (11).

The results are shown in Fig. 7. In Fig. 7(a), we show the results without form factors with $g_{K^*N\Theta} < 0$, where the t and s channels interfere constructively. Given in Fig. 7(d) are the results with $g_{K^*N\Theta} > 0$, where we have destructive interference. In these plots, we give the results by varying the value of $g_{K^*N\Theta}$. This evidently shows the important role driven by the t -channel K^* exchange. We see that, even with $g_{K^*N\Theta} = \pm 0.5$, K^* exchange cannot be neglected. This can be seen by comparing with the results of the s -channel alone (the dot-dashed lines). In Figs. 7(b,e), we show the results with the form factor of Eq. (20). Following Ref. [41], we use Λ

= 0.5 GeV. Here again the role of K^* exchange can be easily found. In this reaction, we also found that the form factor (20) suppresses the cross section by an order of magnitude, which is due to the soft cutoff value. If we use $\Lambda = 0.75$ GeV in Eq. (20), the peak value in Fig. 7(b) would be 0.6 mb. The effect of the K^* exchange is even more drastic when we use the form factor of Eq. (21). Figures 7(c,f) show our results with the form factor of Eq. (21) and $\Lambda = 1.8$ GeV. Here the results without the K^* exchange is very much suppressed with the peak value being only about 25 μ b. But with the K^* exchange the cross sections become a few hundred μ b depending on the magnitude of $g_{K^*N\Theta}$. We also found that the cross sections are not so sensitive to the phase of $g_{K^*N\Theta}$, thus the $\pi^- p \rightarrow K^- \Theta^+$ reaction can be a good place to measure its magnitude.

IV. PRODUCTION OF NEGATIVE-PARITY Θ^+

We now consider the production of Θ^+ assuming that it has negative parity. This process was considered in Ref. [43] for the photon-neutron reaction and was found to have smaller cross sections than the positive-parity Θ^+ production. In this case, the effective Lagrangians in Eqs. (1) and (2) are changed as

$$\begin{aligned} \mathcal{L}_{K^*N\Theta} &= g_{K^*N\Theta}(\bar{\Theta} K^+ n - \bar{\Theta} K^0 p) + \text{H.c.}, \\ \mathcal{L}_{K^*N\Theta} &= -ig_{K^*N\Theta}(\bar{\Theta} \gamma_5 \gamma^\mu K_\mu^{*+} n - \bar{\Theta} \gamma_5 \gamma^\mu K_\mu^{*0} p) + \text{H.c.}, \end{aligned} \quad (22)$$

where we have dropped the tensor coupling terms of the $K^*N\Theta$ interaction as its effects will not be considered

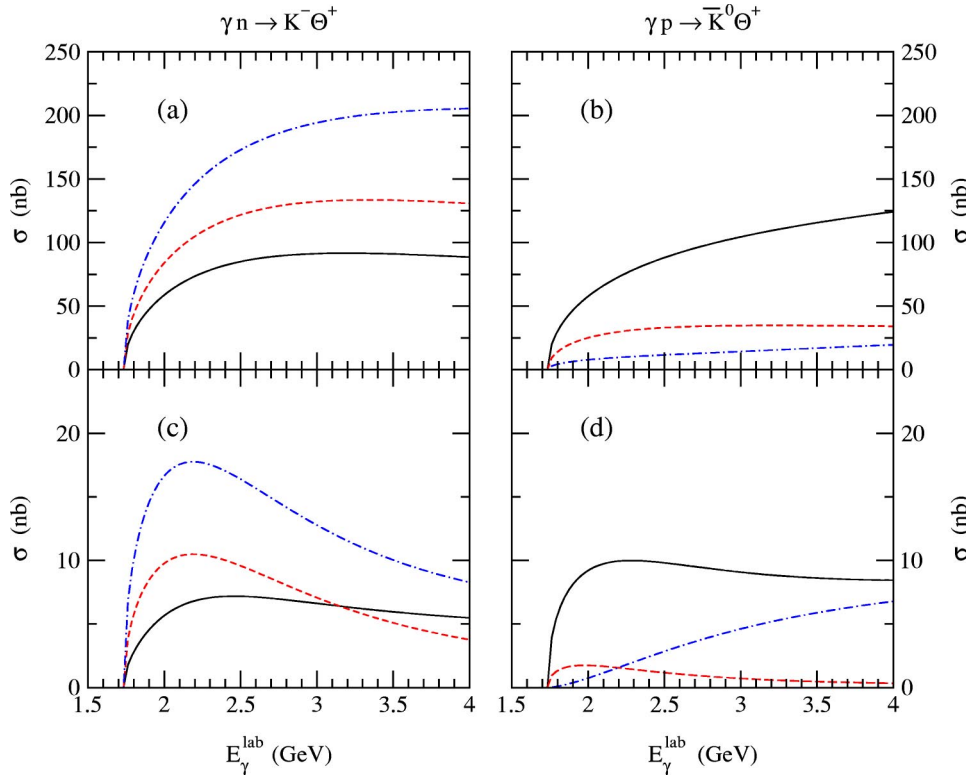


FIG. 8. Cross sections for (a,c) $\gamma n \rightarrow K^- \Theta^+$ and (b,d) $\gamma p \rightarrow \bar{K}^0 \Theta^+$ when the Θ^+ has negative parity. In (a,b) no form factors are used and in (c,d) the form factors (11) are used with $\Lambda = 1.8$ GeV. The solid lines are the results with $g_{K^*N\Theta} = g_{KN\Theta}$, the dashed lines with $g_{K^*N\Theta} = 0$, and the dot-dashed lines with $g_{K^*N\Theta} = -g_{KN\Theta}$.

throughout this work. The form of the above effective Lagrangians is obtained with the prescription of Ref. [63], which was used to construct the effective Lagrangians for the interactions of the $J^P = \frac{1}{2}^-$ $S_{11}(1535)$ resonance. Here we inserted $i\gamma_5$ in the appropriate place in order to account for the odd parity of the Θ^+ . Then the decay width of $\Theta^+ \rightarrow KN$ becomes

$$\Gamma_{\Theta^+ \rightarrow K^+ n + K^0 p} = \frac{g_{KN\Theta}^2}{2\pi} \frac{|\mathbf{p}_K|(\sqrt{M_N^2 + \mathbf{p}_K^2} + M_N)}{M_\Theta}, \quad (23)$$

which gives $g_{KN\Theta} = 0.307$ with $\Gamma_\Theta = 5$ MeV.

The production amplitudes for $\gamma n \rightarrow K^- \Theta^+$ are

$$\begin{aligned} \mathcal{M}_{1(a)}^\mu &= \frac{eg_{KN\Theta}(2q^\mu - k^\mu)}{t - M_K^2} F_{1(a)}(s, t, u), \\ \mathcal{M}_{1(b)}^\mu &= \frac{i g_{K^*K\gamma} g_{K^*N\Theta}}{t - M_{K^*}^2} \epsilon^{\mu\nu\alpha\beta} k_\alpha q_\beta \gamma_5 \gamma_\nu F_{1(b)}(s, t, u), \\ \mathcal{M}_{1(c)}^\mu &= -\frac{ie\kappa_n}{2M_N} \frac{g_{KN\Theta}}{s - M_N^2} (k + p + M_N) \sigma^{\mu\nu} k_\nu F_{1(c)}(s, t, u), \\ \mathcal{M}_{1(d)}^\mu &= -\frac{eg_{KN\Theta}}{u - M_\Theta^2} \left(\gamma_\mu + \frac{i\kappa_\Theta}{2M_\Theta} \sigma^{\mu\nu} k_\nu \right) \\ &\quad \times (p - q + M_\Theta) F_{1(d)}(s, t, u). \end{aligned} \quad (24)$$

For $\gamma p \rightarrow \bar{K}^0 \Theta^+$ we have

$$\begin{aligned} \mathcal{M}_{2(a)}^\mu &= -\frac{ig_{K^*K\gamma} g_{K^*N\Theta}}{t - M_{K^*}^2} \epsilon^{\mu\nu\alpha\beta} k_\alpha q_\beta \gamma_5 \gamma_\nu F_{2(a)}(s, t, u), \\ \mathcal{M}_{2(b)}^\mu &= \frac{eg_{KN\Theta}}{s - M_N^2} (k + p + M_N) \left(\gamma_\mu + \frac{i\kappa_p}{2M_N} \sigma^{\mu\nu} k_\nu \right) \\ &\quad \times F_{2(b)}(s, t, u), \\ \mathcal{M}_{2(c)}^\mu &= \frac{eg_{KN\Theta}}{u - M_\Theta^2} \left(\gamma_\mu + \frac{i\kappa_\Theta}{2M_\Theta} \sigma^{\mu\nu} k_\nu \right) (p - q + M_\Theta) \\ &\quad \times F_{2(c)}(s, t, u), \end{aligned} \quad (25)$$

and the $\pi^- p \rightarrow K^- \Theta^+$ process has

$$\begin{aligned} \mathcal{M}_{6(a)} &= -\frac{i\sqrt{2}g_{K^*K\pi}g_{K^*N\Theta}}{t - M_{K^*}^2} \\ &\quad \times \left\{ k + q + \frac{M_K^2 - M_\pi^2}{M_{K^*}^2} (k - q) \right\} \gamma_5 F_{6(a)}(s, t, u), \\ \mathcal{M}_{6(b)} &= -\frac{i\sqrt{2}g_{KN\Theta}g_{\pi NN}}{s - M_N^2} (k + p + M_N) \gamma_5 F_{6(b)}(s, t, u). \end{aligned} \quad (26)$$

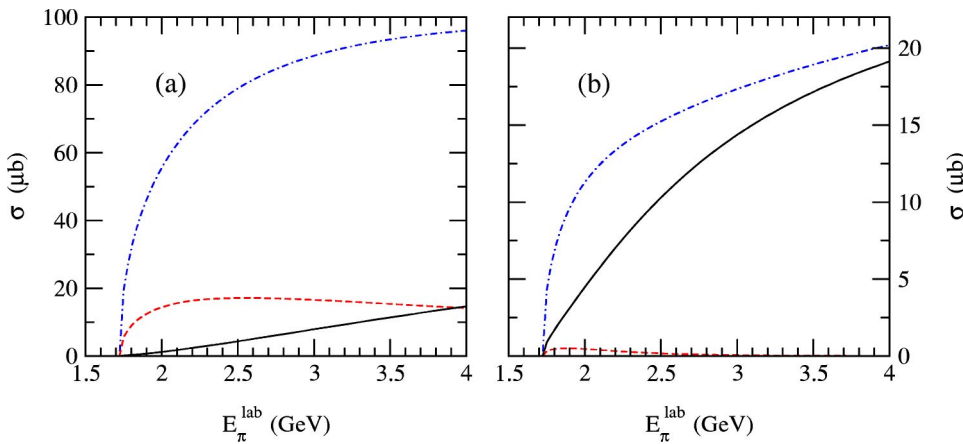


FIG. 9. Cross sections for $\pi^- p \rightarrow K^- \Theta^+$ when the Θ^+ has negative parity. In (a) no form factors are used and in (b) the form factors (11) are used with $\Lambda = 1.8$ GeV. The notations are the same as in Fig. 8.

The results are given in Figs. 8 and 9 with $g_{K\Theta} = 0.307$. Given in Fig. 8 are the photon-neutron and photon-proton reaction results and the pion-proton reaction results are shown in Fig. 9. In these figures the solid lines are obtained with $g_{K^*N\Theta} = g_{K\Theta}$, the dashed lines are with $g_{K^*N\Theta} = 0$, and the dot-dashed lines are with $g_{K^*N\Theta} = -g_{K\Theta}$. Here we set $\kappa_\Theta = 0$. In Ref. [43], it is claimed that the cross section for the negative-parity Θ^+ is suppressed compared with the positive-parity Θ^+ in the case of photon-neutron reaction. We confirmed this conclusion and found that this is true not only in the photon-neutron reaction, but also in photon-proton and pion-proton reactions. In photoproduction, the cross sections are small, less than 200 nb even without form factors, and the cross section for the photon-neutron reaction is slightly larger than that for the photon-proton reaction. If the form factors of Eq. (11) are used with $\Lambda = 1.8$ GeV, the cross sections become less than 20 nb. Therefore this seems to be inconsistent with the SAPHIR observation that the cross section for the photon-proton reaction is about 200 nb. The suppression of the cross section is also seen in the case of the pion-proton reaction (Fig. 9). In this reaction, the cross section for the negative-parity Θ^+ is less than 100 μb without form factors and less than 20 μb with the form factors. Thus precise measurements on the production processes may distinguish the parity of the Θ^+ baryon.

V. SUMMARY AND DISCUSSION

We have investigated the production processes of the exotic Θ^+ , which was discovered recently by several experiments. We considered photon-induced production reactions, which were used in the experiments of the LEPS Collaboration, CLAS Collaboration, and SAPHIR Collaboration. In addition, we have considered pion-induced production, which is used by the current KEK experiments and is also available at GSI.

Previous analyses on these reactions [41–43] are improved and extended by including some missing interactions and K^* exchanges. We also employ the form factors and cutoff parameters motivated by the study of Λ photoproduction. Our results show that the photon-proton reaction cross section is somehow larger than that of the photon-neutron

reaction. This is in contrast to the conclusion of Refs. [41,42], which predicted a larger cross section for the photon-neutron reaction. This is mainly because the model of Refs. [41,42] does not include the tensor coupling of the electromagnetic interactions and the K^* exchanges were not coherently included in both reactions. The cross sections of the two reactions, photon-neutron and photon-proton reactions, are in the range of a few hundred nb, which seems to be consistent with the SAPHIR observation as far as photon-proton reaction is concerned. But they have different energy dependence which should be verified by experiments and can test the models adopted in this study. Furthermore, the SAPHIR Collaboration claimed that the cross section of $\gamma p \rightarrow \bar{K}^0 \Theta^+$ is similar to that of $\gamma p \rightarrow \phi p$. If this is confirmed, the positive phase of the $g_{K^*N\Theta}$ seems to be favored. [See Fig. 5(b).]

The pion-induced reaction has a much larger cross section than the photon-induced reactions. We found that this reaction is very sensitive to the magnitude of the $K^*N\Theta$ coupling but not so to its phase. So measurement of this reaction would give us a guide to estimate the magnitude of $g_{K^*N\Theta}$. Due to lack of information, we could not investigate the role of the tensor couplings of the $K^*N\Theta$ interaction and the role of nucleon resonances like the nucleon analog of the Θ^+ in the s channels. Therefore, theoretical studies on the Θ couplings in various models are highly desirable and useful to understand the structure and the production mechanisms of the Θ^+ .

Since we are employing covariant form factors which are different from the form factors used in previous studies [41–43], it will be useful to measure differential cross sections, which will discriminate between different form factors. In Fig. 10, we give our predictions on the differential cross sections for $\gamma n \rightarrow K^- \Theta^+$, $\gamma p \rightarrow \bar{K}^0 \Theta^+$, and $\pi^- p \rightarrow K^- \Theta^+$ with the photon or pion energy at 2.5 GeV, where the scattering angle θ is defined by the directions of the initial photon (pion) momentum and the final K meson momentum in the c.m. frame. The solid, dotted, and dashed lines are obtained with $g_{K^*N\Theta} = g_{K\Theta}$, $g_{K^*N\Theta} = 0$, and $g_{K^*N\Theta} = -g_{K\Theta}$, respectively, where $g_{K\Theta} = 2.2$. This shows that the differential cross section for $\pi^- p \rightarrow K^- \Theta^+$ has a forward peak, which is due to the dominance of the K^* exchange. In photoproduction, the differential cross section is suppressed

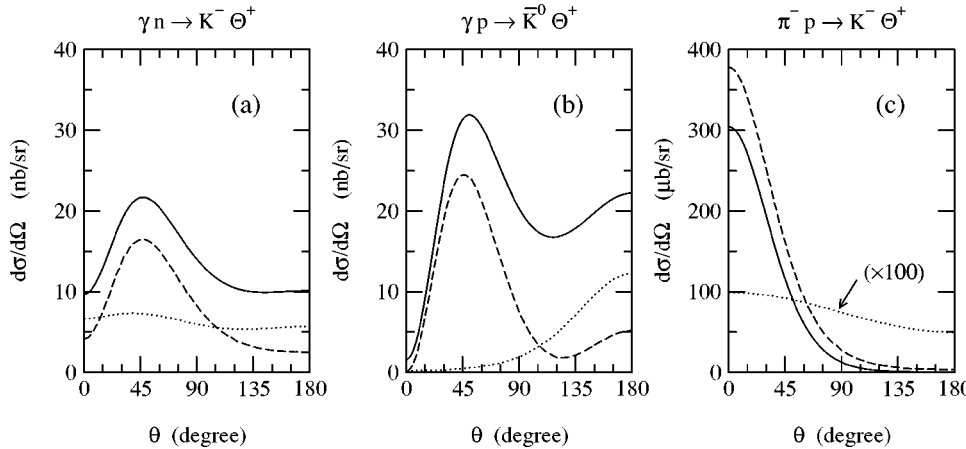


FIG. 10. Differential cross sections for (a) $\gamma n \rightarrow K^- \Theta^+$ at $E_\gamma^{\text{lab}} = 2.5$ GeV, (b) $\gamma p \rightarrow \bar{K}^0 \Theta^+$ at $E_\gamma^{\text{lab}} = 2.5$ GeV, and (c) $\pi^- p \rightarrow K^- \Theta^+$ at $E_\pi^{\text{lab}} = 2.5$ GeV, when the Θ^+ has positive parity. The form factors (11) are used with $\Lambda = 1.8$ GeV. The solid, dotted, and dashed lines are obtained with $g_{K^*N\Theta} = g_{K N\Theta}$, $g_{K^*N\Theta} = 0$, and $g_{K^*N\Theta} = -g_{K N\Theta}$, respectively, where $g_{K N\Theta} = 2.2$. In (c), the dotted line is scaled by a factor of 100.

at forward angles and the peak is at $\theta \sim 45^\circ$. In particular, a backward (secondary) peak is observed in the case of the photon-proton reaction.

Finally, we have also investigated the production processes of negative-parity Θ^+ since several studies claim that the Θ^+ has odd parity. We found that the cross sections in this case are very much suppressed compared with the positive-parity Θ^+ case. Thus the interpretation of the Θ^+ as an odd parity pentaquark state seems to be disfavored by the SAPHIR observation, which claims that the cross section for the photon-proton reaction is about 200 nb. So if the SAPHIR results are confirmed by other experiments, the in-

terpretation of the Θ^+ as an $I=0$ and $J^P=\frac{1}{2}^+$ pentaquark will be strongly supported. Most importantly, further experimental measurements are crucial to make any decisive conclusion on the couplings and the structure of the Θ^+ .

ACKNOWLEDGMENTS

We are grateful to J. Barth, N. I. Kochelev, T. Nakano, and T.-S. H. Lee for useful information and fruitful discussions. This work was supported by Korea Research Foundation Grant (KRF-2002-015-CP0074).

[1] LEPS Collaboration, T. Nakano *et al.*, Phys. Rev. Lett. **91**, 012002 (2003).
[2] CLAS Collaboration, S. Stepanyan *et al.*, hep-ex/0307018.
[3] SAPHIR Collaboration, J. Barth *et al.*, Phys. Lett. B **572**, 127 (2003).
[4] DIANA Collaboration, V.V. Barmin *et al.*, Yad. Fiz. **66**, 1763 (2003) [Phys. At. Nucl. **66**, 1715 (2003)].
[5] A.E. Asratyan, A.G. Dolgolenko, and M.A. Kubantsev, hep-ex/0309042.
[6] D. Diakonov, V. Petrov, and M. Polyakov, Z. Phys. A **359**, 305 (1997).
[7] M. Chemtob, Nucl. Phys. **B256**, 600 (1985).
[8] H. Weigel, Eur. Phys. J. A **2**, 391 (1998).
[9] M. Praszałowicz, hep-ph/0308114.
[10] M. Karliner and H.J. Lipkin, hep-ph/0307343.
[11] R. Jaffe and F. Wilczek, Phys. Rev. Lett. **91**, 232003 (2003).
[12] K. Cheung, hep-ph/0308176.
[13] C. Gignoux, B. Silvestre-Brac, and J.M. Richard, Phys. Lett. B **193**, 323 (1987); H.J. Lipkin, *ibid.* **195**, 484 (1987).
[14] D.O. Riska and N.N. Scoccola, Phys. Lett. B **299**, 338 (1993).
[15] Y. Oh, B.-Y. Park, and D.-P. Min, Phys. Lett. B **331**, 362 (1994); Phys. Rev. D **50**, 3350 (1994).
[16] Y. Oh and B.-Y. Park, Phys. Rev. D **51**, 5016 (1995).
[17] E791 Collaboration, E.M. Aitala *et al.*, Phys. Rev. Lett. **81**, 44 (1998); Phys. Lett. B **448**, 303 (1999).
[18] F.I. Stancu and D.O. Riska, hep-ph/0307010.
[19] C.E. Carlson, C.D. Carone, H.J. Kwee, and V. Nazaryan, Phys. Lett. B **573**, 101 (2003).
[20] L.Ya. Glozman, Phys. Lett. B **575**, 18 (2003); hep-ph/0309092.
[21] M. Karliner and H.J. Lipkin, hep-ph/0307243.
[22] H. Walliser and V.B. Kopeliovich, hep-ph/0304058.
[23] B.K. Jennings and K. Maltman, hep-ph/0308286.
[24] D. Borisyuk, M. Faber, and A. Kobushkin, hep-ph/0307370.
[25] N. Itzhaki, I.R. Klebanov, P. Ouyang, and L. Rastelli, hep-ph/0309305.
[26] S.-L. Zhu, hep-ph/0307345.
[27] R.D. Matheus, F.S. Navarra, M. Nielsen, R. da Silva, and S.H. Lee, Phys. Lett. B (to be published), hep-ph/0309001.
[28] J. Sugiyama, T. Doi, and M. Oka, hep-ph/0309271.
[29] A. Hosaka, Phys. Lett. B **571**, 55 (2003).
[30] T.D. Cohen, hep-ph/0309111; T.D. Cohen and R.F. Lebed, hep-ph/0309150.
[31] F. Csikor, Z. Fodor, S.D. Katz, and T.G. Kovács, hep-lat/0309090; S. Sasaki, hep-lat/0310014.
[32] B.G. Wybourne, hep-ph/0307170.
[33] J. Randrup, Phys. Rev. C **68**, 031903 (2003).
[34] L.W. Chen, V. Greco, C.M. Ko, S.H. Lee, and W. Liu, nucl-th/0308006.
[35] P. Bicudo and G.M. Marques, hep-ph/0308073.
[36] S. Capstick, P.R. Page, and W. Roberts, Phys. Lett. B **570**, 185 (2003).
[37] T. Hyodo, A. Hosaka, and E. Oset, nucl-th/0307105.
[38] M.V. Polyakov and A. Rathke, hep-ph/0303138.
[39] X. Chen, Y. Mao, and B.-Q. Ma, hep-ph/0307381.
[40] H. Gao and B.-Q. Ma, Mod. Phys. Lett. A **14**, 2313 (1999).

- [41] W. Liu and C.M. Ko, Phys. Rev. C **68**, 045203 (2003).
- [42] W. Liu and C.M. Ko, nucl-th/0309023.
- [43] S.I. Nam, A. Hosaka, and H.-C. Kim, hep-ph/0308313.
- [44] J. Barth (private communication).
- [45] C.E. Carlson, C.D. Carone, H.J. Kwee, and V. Nazaryan, hep-ph/0310038.
- [46] Y. Oh, H. Kim, and S.H. Lee, hep-ph/0310117.
- [47] M.V. Polyakov, A. Sibirtsev, K. Tsushima, W. Cassing, and K. Goeke, Eur. Phys. J. A **9**, 115 (2000).
- [48] S. Nussinov, hep-ph/0307357.
- [49] R.A. Arndt, I.I. Strakovsky, and R.L. Workman, Phys. Rev. C **68**, 042201 (2003).
- [50] A. Casher and S. Nussinov, hep-ph/0309208.
- [51] J. Haidenbauer and G. Krein, Phys. Rev. C **68**, 052201 (2003).
- [52] S. Janssen, J. Ryckebusch, W. Van Nespen, D. Debruyne, and T. Van Cauteren, Eur. Phys. J. A **11**, 105 (2001).
- [53] H.-C. Kim, hep-ph/0308242.
- [54] Particle Data Group, K. Hagiwara *et al.*, Phys. Rev. D **66**, 010001 (2002).
- [55] R.L. Workman and H.W. Fearing, Phys. Rev. D **37**, 3117 (1988).
- [56] T. Mart and C. Bennhold, Phys. Rev. C **61**, 012201 (2000).
- [57] B.S. Han, M.K. Cheoun, K.S. Kim, and I.-T. Cheon, Nucl. Phys. **A691**, 713 (2001).
- [58] B.C. Pearce and B.K. Jennings, Nucl. Phys. **A528**, 655 (1991).
- [59] K. Ohta, Phys. Rev. C **40**, 1335 (1989).
- [60] H. Haberzettl, C. Bennhold, T. Mart, and T. Feuster, Phys. Rev. C **58**, 40 (1998).
- [61] R.M. Davidson and R. Workman, Phys. Rev. C **63**, 025210 (2001); **63**, 058201 (2001).
- [62] Y. Oh, A. I. Titov, and T.-S. H. Lee, in *NSTAR2000 Workshop: Excited Nucleons and Hadronic Structure*, edited by V. D. Burkert, L. Elouadrhiri, J. J. Kelly, and R. C. Minehart (World Scientific, Singapore, 2000), pp. 255–262.
- [63] M. Benmerrouche, N.C. Mukhopadhyay, and J.F. Zhang, Phys. Rev. D **51**, 3237 (1995).